Using the resistivity method for leakage detection in a blind test at the Rossvatn embankment dam test facility in Norway

Sjodahl, P.; Dahlin, Torleif; Johansson, S.

Published in:
Bulletin of Engineering Geology and the Environment

DOI:
10.1007/s10064-010-0314-y

2010

Bull Eng Geol Environ (2010) 69:643–658
DOI 10.1007/s10064-010-0314-y

ORIGINAL PAPER

Using the resistivity method for leakage detection in a blind test at the Røssvatn embankment dam test facility in Norway

P. Sjödahl · T. Dahlin · S. Johansson

Received: 8 March 2008 / Accepted: 21 July 2010 / Published online: 27 August 2010

Abstract Internal erosion is a cause of embankment dam failure, thus it is important to develop methods for seepage monitoring and internal erosion detection. In order to evaluate the potential of resistivity monitoring to give an early warning of such leakage/erosion, a test was undertaken on a rockfill embankment dam with a central glacial till core at the Røssvatn test facility in Norway. Three defects, consisting of permeable material, were built into the dam at various depths and locations unknown to the personnel carrying out the measurements and data interpretation. A numerical modelling pre-study was carried out, showing that all the actually constructed defects were too small to be detected by single time investigation. In the final test, repeated measurements were undertaken with different reservoir levels, i.e. a limited monitoring approach. This increased the detection capability, confirming the value of the geophysical approach and that monitoring is superior to single time investigations.

Keywords Resistivity · Modelling · Embankment dam · Internal erosion · Leakage · Seepage detection

Résumé L'érosion interne est une cause de rupture des barrages en terre, de sorte qu'il est important de développer des méthodes pour surveiller les écoulements et détecter l'érosion interne. Afin d'évaluer le potentiel des méthodes de résistivité électrique pour donner une alerte précoce de ces phénomènes, un test a été entrepris sur un barrage en enrochement comportant un noyau central de moraine glaciaire sur la station d'essai de Rossvatn en Norvège. Trois défauts, réalisés à partir de matériaux perméables, ont été mis en place dans le barrage à différentes profondeurs et en des endroits non connus des personnes réalisant les mesures et l'interprétation des données. Une pré-étude par simulation numérique a été réalisée, montrant que tous les défauts mis en place étaient trop petits pour être détectés par des investigations isolées. Dans le test final, des mesures répétées ont été réalisées avec différents niveaux de réservoir, i.e. suivant une approche par surveillance. Ceci a augmenté les possibilités de détection, confirmant la valeur d'une approche géophysique et l'intérêt d'une surveillance par rapport à des investigation isolées.

Mots clés Résistivité · Modélisation · Barrage en terre · Erosion interne · Fuite · Détection d'écoulement

P. Sjödahl (✉) · S. Johansson
HydroResearch Sam Johansson AB,
Stora Marknadsvägen 15 S Vpl 12,
183 34 Täby, Sweden
e-mail: pontus.sjodahl@hydroresearch.se

T. Dahlin
Engineering Geology, Lund University,
Box 118, 221 00 Lund, Sweden

Introduction

Methods for seepage monitoring and internal erosion detection give essential information for the safety evaluation of earth embankment dams. Experiences from dam safety work indicate that the use of existing methods is in many cases insufficient, and there is a considerable need for improved surveillance on dams worldwide. Like any other construction, dams age and need rehabilitation. In Sweden the average dam was built in the late 1950s, and the situation is similar in many other parts of the world (ICOLD 1998). As a consequence, there is an increasing need for dam surveillance in the future.

The increased concern with the safety of aging dams has resulted in new standards and dam safety guidelines

emerging all over the world while technical improvements facilitate data acquisition in existing monitoring systems and make new systems more efficient. In addition to a high demand for conventional monitoring of dams, there is an intensified interest in new and non-conventional methods. One sign of this increased interest is the industries' willingness to support the testing of some unconventional methods at an embankment dam test facility in Norway, on which this study is based.

For embankment dams the main concern is to keep track of the seepage. With the exception of overtopping, internal erosion through the dam or the foundation is the most frequent reason for embankment dam failures (ICOLD 1995; Foster et al. 2000a). While overtopping scenarios might be difficult to predict, they are at least easy to understand and design surveillance systems for. An efficient surveillance system for internal erosion monitoring, on the other hand, is far more complicated.

Internal erosion in the embankment or in the foundation of the dam has progressed considerably before any evidence is seen on the outside of the dam. Early warnings are typically higher seepage rates or even a visually observable concentrated leak at the downstream toe. High turbidity of seepage water is another sign. Such a development may in some cases heal by itself when material from the upstream filter enters into the core, thereby reducing seepage rates. This process of increasing seepage followed by self-healing may repeat itself, and last for several years. In time the process will approach the crest of the dam, as material from the overlying parts of the dam will repeatedly drop, resulting in a new damage zone located on a higher level. Finally, when the process reaches the dam surface it will appear as a sinkhole. However, an embankment dam failure caused by internal erosion may also occur quite abruptly. The period between an early warning of a concentrated leak at the downstream toe to a full dam failure at the crest may be just a few hours (Foster et al. 2000b; Fell et al. 2003). Seepage monitoring systems with higher accuracy and improved special resolution are therefore of great value as they may extend the time frame between an early warning and a possible failure.

Conventional methods of detecting internal erosion consist typically of monitoring of seepage, pore pressure measurements and visual inspections at the dam. Sometimes turbidity of seepage water is measured. In a scenario where internal erosion develops rapidly, within hours, it is highly unlikely that any conventional method will discover the process in time to avoid a failure. In an attempt to improve surveillance systems unconventional methods are sometimes applied, but so far mostly on a research basis. Temperature measurements, resistivity measurements and self-potential (SP) measurements are three such methods chosen for this study.

Temperature measurements have proved a powerful method for detecting high seepages in embankments (e.g. Dornstädter 1997; Johansson 1991; Johansson 1997; Kappelmeyer 1957; Merkler et al. 1985). The technique makes use of the fact that increased seepage affects the temperature pattern in the dam. This temperature effect can be measured and related to seepage rates. New improved possibilities of measuring temperature using optical fibre sensors further increase the capability of the method.

Resistivity is a well-established technique for a broad variety of purposes in engineering and environmental ground investigations. It has been used for leakage detection on many occasions, with mixed results (e.g. Buselli and Lu 2001; Butler and Llopis 1990; Panthulu et al. 2001; Sjödahl et al. 2005; Titov et al. 2000; Van Tuyen et al. 2000). A more effective, but more demanding, approach is to carry out repeated measurements or long-term monitoring (Johansson and Dahlin 1996; Johansson et al. 2005a).

Self-potential measurements have long been considered especially interesting for dam seepage investigations, where it has been frequently used (e.g. Butler and Llopis 1990; Corwin and Butler 1989; Ogilvy et al. 1969; Triumf and Thunehed 1996; Wilt and Corwin 1988). The main reason for this particular interest is the method's natural physical coupling to subsurface water flow. As with resistivity, SP can be used both in single investigations and in long-term monitoring.

All three methods (resistivity, self-potential and temperature) are indirect methods for detecting leakage by monitoring embankment dams. The interpretation of the results is often uncertain, and should if possible be supported with measurements from other methods. Unfortunately, this is often difficult on dams as instrumentation is sparse and intrusive methods such as drilling are usually avoided.

This paper reports the finding of investigations on an embankment dam using the resistivity method. A summary of the results obtained using other methods was reported by Johansson et al. (2005b).

The Røssvatn test dam facility

The embankment dam test site is located in Norway, around 60 km south of the town of Mo i Rana and close to the large Røssvatn reservoir (Fig. 1). Beginning in 2001, a series of stability and breaching tests has been carried out at this unique test site. Numerous dams some 5–6 m in height and approximately 40 m in length have been built using different materials and designs and then forced to failure. All the tests were thoroughly documented in order to increase understanding of the stability of embankment dams and to analyse real dam failure scenarios (Høeg et al. 2004).

Fig. 1 Aerial photograph of the location of the embankment test facility in Røssåga river. In the *upper left part* is the Røssvatn reservoir impounded by the Røssvassdamen dam (from Høeg et al. 2004)

The test site is located on the Røssåga River, about 600 m downstream of the Røssvassdammen dam which impounds the large Røssvatn reservoir. Water is discharged to the Upper Røssåga power plant through an underground intake tunnel. The Røssåga River is normally dry, except for some limited local flow and occasional discharge during flooding situations, typically in springtime. The chosen location in the Røssåga River has a well-defined bedrock foundation and sharp abutments making it suitable for the tests. In addition, water can easily be discharged by regulating one or more of the three spillway gates in the Røssvassdammen dam such that the small reservoir at the test site can be raised in a controlled manner. Furthermore, with a spillway gate capacity of 450 m^3/s, it is possible to maintain a constant reservoir level even after the breaching of the dam has commenced.

Arrangement of the blind test

Although the purpose of the research program was to study the breaching of embankment dams, additionally leakage detection methods would be undertaken on one of the test embankments provided it did not interfere with the main purpose of the field tests. This smaller project to test the performance of some unconventional leakage and internal erosion detection at the test site included measurements on one of the planned test embankments (referred to as 1-2003) which was redesigned and constructed with some well-defined defects inbuilt into the core of the dam.

The monitoring was intended to evaluate some different techniques to detect leakages and internal erosion in full-scale embankment dams, identifying their ranges and capabilities. While various similar tests have been performed at the laboratory scale, large controlled field tests are rare. Armbruster et al. (1989) carried out seepage investigations on a 3.6 m high embankment dam model. They concluded temperature measurements and to some degree also SP measurements were useful methods for seepage detection. In transferring the results to full-scale dams it should be considered that the resolution capability of resistivity imaging reduces with increasing depth. On the other hand, monitoring on a long-term basis increases the resolution capability through analysis of dynamic processes. In this case, seasonal variations are analyzed, on the assumption that the temperature and total dissolved solids (TDS) of the seepage water may act as natural tracers. Seasonal temperature variation affects the resistivity in a defect area, as well as in a zone around it, thus increasing the size of the target.

In order to be as objective as possible, the personnel involved were separated into different groups. A design group had the task of designing the defects and did not participate in the monitoring while the monitoring group had no knowledge of the locations and sizes of the pre-designed zones of high seepage. The data could then be interpreted without any a-priori information about the defects.

The monitoring group carried out a pre-study on numerical modeling of the embankment to estimate the range in size and location of defects which would be detectable by the SP and resistivity methods. It was also decided to have a systematic visual inspection and to regularly monitor temperature along the downstream toe of the dam. With the results from the pre-study, the dam was constructed in the summer of 2003. Defects, consisting of permeable material, were included in the impervious core. All field measurements were conducted over a period of 9 days immediately after construction ended and the dam was then forced to failure by overtopping. At this time the monitoring group handed in the report with an evaluation of the field data. The results were analyzed internally and the exact location of the defects was made public in late 2004.

Resistivity modelling in the pre-study

Conditions for the pre-study

The resistivity modelling was designed to be as relevant as possible for the actual field experiments, in terms of material properties and geometry. The dam used in the pre-modelling was 40 m long and 5.5 m high (Fig. 2). The upstream and downstream slopes were inclined at 1:1.5. Both the foundation and the steep abutments consisted of solid rock. Direct access to the core was possible during the measurement period; only after all measurements had been

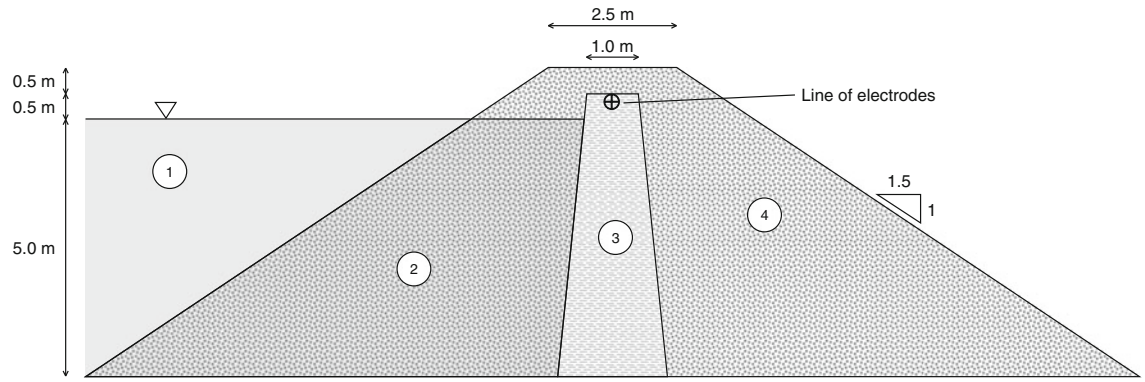

Fig. 2 Cross-section of the dam used for resistivity modelling in the pre-study, with the exception that the core was not covered hence the top 0.5 m is cut off in the dam model. *1* Reservoir water, *2* Upstream rockfill shell, *3* Glacial till core, *4* Downstream rockfill shell. All modelling was done with a full reservoir. The incline of the core was 10:1 and the slope of the upstream and downstream shell 1:1.5

Table 1 Assumed material properties data for the pre-study calculations

Part of dam	Material	Porosity (−)	Resistivity (Ωm)
Pre study	Glacial till	0.18	500
Defect zone	Sand/gravel	0.25–0.31	2100–2800
Support fill (downstream)	Rockfill A	0.35	20000
Support fill (upstream)	Rockfill B	0.35	1700
Foundation and abutments	Bedrock	–	20000
Reservoir	Water	–	400

taken was the last 0.5 m of rockfill placed over the top of the core.

Data on the electrical properties of earth- and rockfill embankment construction materials are surprisingly rare, which is a serious problem when evaluating the capabilities of the resistivity method. The values used in this study (Table 1) were based on data from the literature (Schopper 1982; Schön 1996) and information from dam monitoring experiences in Sweden. High resistivity (several hundreds of Ωm) reservoir water has been measured in rivers in northern Sweden (Johansson et al. 2005a). The resistivity of the water influences the resistivity of the soils. Assuming all electrical conduction is taking place in the pore fluid, the soil resistivities can be roughly calculated using porosity estimates (Table 1) based on the relation given by Archie (1942) for saturated soils.

Both the rockfill washed downstream and the bedrock foundation would be expected to have very high resistivities whereas for the core, with a significant content of fines, the Archie relation is not applicable. For this material, different models have been developed based on conduction in two phases: through the pore fluid and along the particle surfaces. However, resistivities around a few hundred Ωm have been established for Swedish fine-grained tills (Bergström 1998; Johansson et al. 2005b). Modelling was carried out assuming different values for the defect materials, depending on grain size and porosity. All results obtained in this study indicated a resistivity of 2,800 Ωm for the materials constituting the defects. It is appreciated that there could be large variations in these parameters, but unfortunately a full laboratory test programme could not be undertaken. Although a few preliminary investigations were performed at a later stage, they did not influence the work conducted in the pre-study period.

In order to estimate what kind of defects could be detected, a sensitivity analysis was carried out. A combination of different defect parameters were assessed with calculations made for defect centres at 1, 3 and 5 m depth. In all situations a full reservoir level (0.5 m below the crest) was assumed. The size, i.e. the cross-sectional area, of the damage was also varied in the calculations. Two different sizes were chosen, medium and large, with cross-sectional areas of 0.25 and 1.0 m^2 respectively. A small size and an extra large size were originally tested, but the small one was quickly found to be undetectable at all depths and the extra large size was considered unrealistic in relation to the size of the dam. The shape of the cross-section of the defect was also considered but found to have little influence on the results. As a consequence, the experiments used square-shaped defects, although flat and wide defects might be more realistic as dams are constructed in layers and hence a certain layer could demonstrate particular weakness.

Modelling principles

The simulated measurements in the resistivity modelling study were selected to reflect the actual field experiments. In the field, measuring was to be carried out as

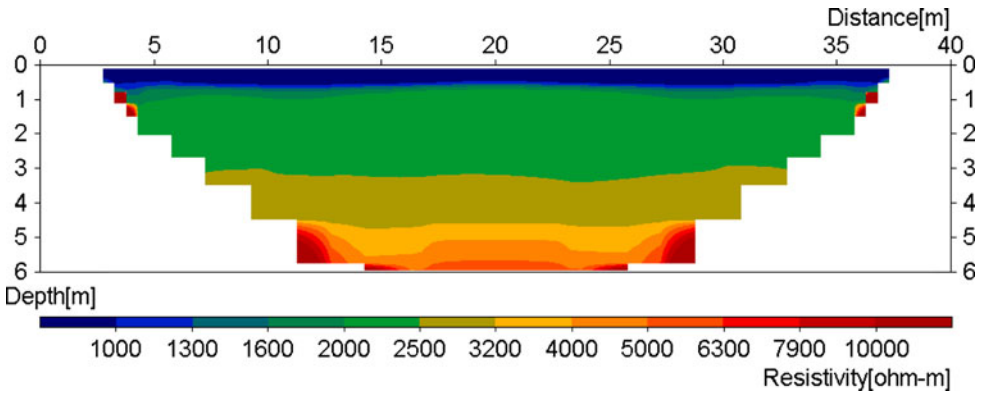

Fig. 3 Inverted model for the "healthy" dam with no defects (mean residual 2.5%)

two-dimensional (2D) resistivity imaging with electrodes installed along the crest of the dam. This is the most convenient way to arrange the electrodes, and the most relevant as it is often the only practical option for monitoring installation in existing dams. There were 518 individual measurements, using a gradient array. While a few different electrode arrays were planned for the field measurements, the pre-study was limited to the use of the gradient array. Previous studies have shown that the gradient array demonstrates reliable results (Dahlin and Zhou 2005). A minimum electrode spacing of 1 m was used.

In order to assess the resolution capability of the measurement concept outlined above, three-dimensional (3D) forward numerical modelling of resistivity measurements was carried out using software developed by Dr. Bing Zhou at the University of Adelaide, Australia (Zhou and Greenhalgh 2001). This uses the finite element method to calculate the full three-dimensional potential field for any defined geological model. Apparent resistivity values for an arbitrary electrode configuration are given as output.

A geometrical model over the planned dam design was created and the measurement configurations were simulated. The three-dimensional model of the planned embankment construction was built using cell dimensions of (width, length, height) $= (x, y, z) = (0.25, 0.50, 0.25)$ m, resulting in a full model of (82, 82, 23) cells, not including the boundary zones. Boundary conditions are assumed to be regular rock (20000 Ωm) at the foundation and abutments and air elsewhere.

Apparent resistivity values were collected both for the stable dam and for the modelled dams with defects. Anomaly pseudosections were plotted to obtain a rough estimate of the size of the anomaly. The data sets were then inverted using the L1-norm optimisation method (Loke et al. 2003) to estimate true ground resistivities. Inversion was carried out with the commercial software Res2dinv, version 3.52, (Loke 2002) using the same approach as intended for the acquired field data. The inverted data from the stable dam and the dams with built-in defects were compared and the anomaly effect, defined by the change in resistivity due to the simulated defect, was estimated and presented. All defects were located at the midpoint of the section.

Pre-study results

First, simulations were made for a stable dam with no defects. 2D inversion was carried out on the 3D forward model output data. At this stage the geometrical rules for 2D inversion were violated, which leads to distorted depths and erroneous absolute resistivity values. However, to date this is the only feasible way to invert apparent resistivity data from embankment geometries. As can be seen from the 2D inverted dam model (Fig. 3), resistivities increase with depth even though the core is assumed to have a constant resistivity with depth. This is explained by the fact that at greater depths a larger earth volume is involved for the current flow and hence the effect from the embankment slopes and the high-resistivity downstream fill will increase.

Simulations were done for all combinations of defect depth locations, defect geometries and defect materials described above. For the medium sized square-shaped defects the shallowest one, at 1 m depth, was clearly detectable (Fig. 4), whereas no effect was observable from the same defect at the two deeper locations. The large sized square-shaped defects were detectable at all depths, but harder to locate at the greater depths. At 5 m, there is a tendency for the defect area to be smeared out and it was difficult to confidently identify the exact location and even at 3 m there was some distortion (Fig. 5). The impression from the modelling results is that the location is imaged shallower than the real location of the defect. This distortion of vertical location is an example of the consequences of applying 2D inversion on resistivity data from measurements along dam geometries. Prior modelling studies investigated these effects more systematically (Sjödahl et al. 2006). It is something that must be accepted as long as 3D inversion schemes are not available and practically usable.

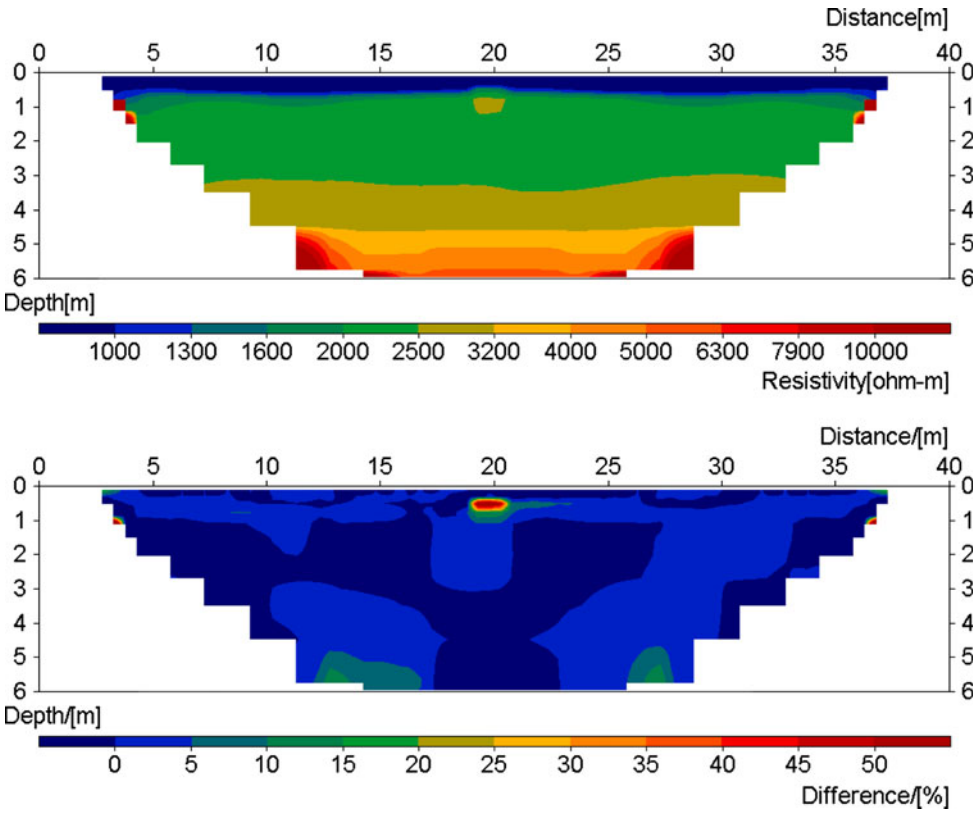

Fig. 4 Inverted model (above) (mean residual 2.4%) and difference model (below) for the medium square defect (0.50 × 0.50 m) located at 1 m depth

Field measurements

The test dam was constructed as a 5.5 m high, 40 m long embankment dam, with a central core of glacial till. The material and geometry were similar to a normal size embankment dam, except that the test dam had no filter zones. The details of the design of the dam, such as bedrock levels, sealing layers and abutments (among others) were not known during the field measurements or during processing and interpretation of the data.

Measurements were made at different reservoir levels starting from an empty reservoir, filling the reservoir completely and emptying it. The filling and emptying of the reservoir was done in steps within a timeframe of 1 week. This progression, with the different time-steps marked out, is described in Fig. 6. Resistivity measurements were taken at all constant reservoir levels and the SP measured during the filling and drainage of the reservoir. The reservoir level was regulated by opening of the spillway gates in the Røssvassdammen dam, situated a few hundred meters upstream. This could quickly fill the reservoir. The reservoir was drained using four outlet pipes, of which two were operated by valves while the other two were equipped with rubber packers. The valves were used in order to keep the water level constant for some hours during the measurements. At the first filling attempt, one of the rubber packers in the drainage pipe failed and the reservoir was emptied.

Data acquisition

The resistivity measurements were carried out as two-dimensional (2D) resistivity imaging with 63 steel electrodes, with a spacing of 0.67 m. The electrodes were installed along the dam crest into the top of the core except for the two last electrodes which were placed outside the dam core (Fig. 7). For the field measurements a modified version of the ABEM Lund Imaging System was used, which includes a Terraohm RIP924 receiver-control unit, an Electrode Selector ES10-64 and a Booster SAS2000 controlled by a field PC. This set-up allows resistivity and induced polarisation (IP) data to be recorded in seven channels simultaneously, leading to fast and efficient data acquisition. Three electrode cables with 21 take-outs each were used to connect the 63 electrodes to the ES10-64.

As the electrodes were installed directly in the dam core, the electrode contact resistances were low and the recorded data stable and of good quality. Initially measurements were repeated for each data point, but as it was hardly ever necessary to go beyond the second value, stacking of data was skipped in order to allow time to try different electrode arrays. The mean variation was below 0.01% for the 1,320

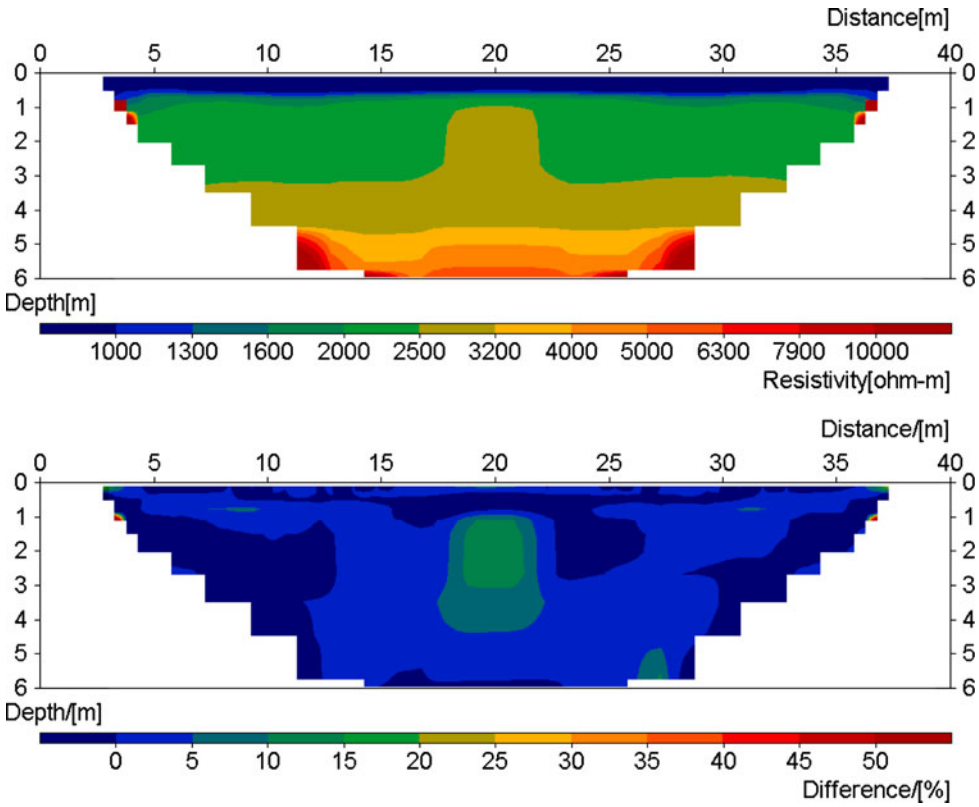

Fig. 5 Inverted model (above) (mean residual 2.4%) and difference model (below) for the large square defect (1.0 × 1.0 m) located at 3 m depth

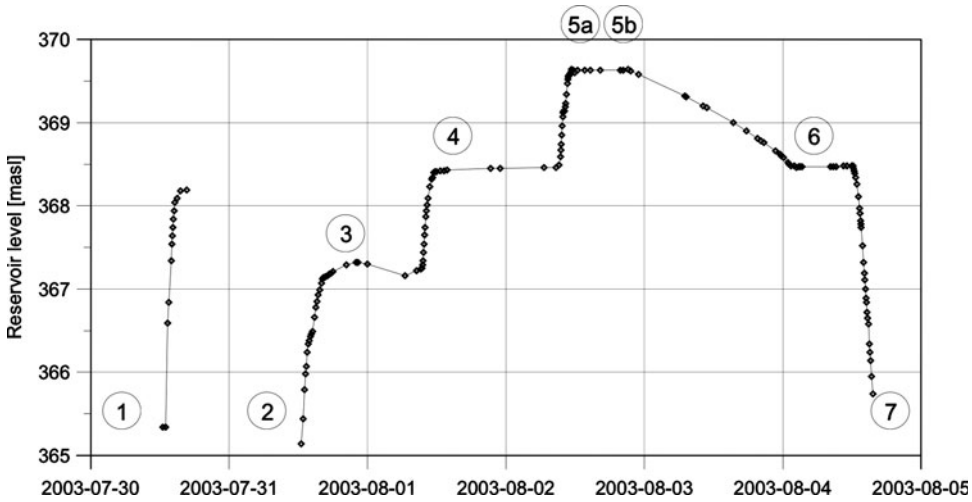

Fig. 6 Filling and emptying of the reservoir. *Numbers* indicate time-steps for resistivity measurements used in this report. Resistivity measurements were taken once or twice on every constant reservoir level, and SP measurements during filling and emptying. The first filling attempt between 1 and 2 failed

data points using the gradient array and slightly higher for the dipole–dipole array with a mean variation around 0.1% and 940 data points. In addition to the gradient and dipole–dipole arrays, pole–dipole and Wenner arrays were also employed, although the latter was only measured for only a few of the time steps.

Previous studies have shown that the gradient array demonstrates reliable results (Dahlin and Zhou 2005). Moreover, it is suitable for field measurements as it can be used with multi-channel equipment making it very efficient. This paper therefore presents the data from the gradient array measurements and one example of joint inversion of gradient and dipole–dipole data.

Data processing and evaluation

The acquired data were analysed through inverse numerical modelling (inversion), using the software Res2dinv, version 3.52 (Loke 2002). The inversion is done through generation of a finite element model of the resistivity distribution in the ground, which is adjusted iteratively to fit the data so that the differences between the model response

Fig. 7 Electrode layout along the dam crest at the Røssvatn test embankment dam, with non-polarising Cu-CuSO4 electrodes for SP monitoring to the *left* and stainless steel electrodes for resistivity and IP monitoring to the *right*

and the measured data (the model residuals) are minimised. This can be done by either minimising the absolute values of the differences (inversion with L1-norm or robust inversion), or minimising the squares of the differences (inversion with L2-norm or smoothness-constrained least-squares inversion) (Loke et al. 2003). Robust (L1-norm) inversion is more capable of handling sharp boundaries in the model and was used for all measurements, due to the expected large contrasts in electrical properties of the materials involved.

Time-lapse inversion was employed to analyse the data from the repeated measurements for change in resistivity. This has the advantage of focussing the results on actual change and suppressing artefacts due to data noise (Loke 2001).

Results from field measurements

In addition to the series of measurements undertaken on the electrode layout installed on the dam crest during the filling and emptying of the reservoir, measurements were extended for 80 m either side of the dam, with a 2 m electrode separation. These were measured with the reservoir empty. The corresponding inverted resistivity sections exhibit large contrasts, where the bottom of the dam stands out as a high resistivity bottom level (several thousand Ωm. Fig. 8). The dam itself exhibits resistivities in the range of a few hundred to a couple of thousand Ωm. The general shape of the bedrock agrees well with the drawings of the dam, with a steep slope to the left and a more gradual incline to the right.

For the layout using the electrodes installed on the dam core, resistivity was measured at a number of different reservoir water levels, from empty to full. The corresponding inverted resistivity sections exhibit large contrasts and significant changes in resistivity are evident as a result of changes in water level. A summary of the results from the field measurements was presented soon after the field survey (Table 2) before the locations of the measuring points were revealed. Three zones were identified as defect areas and another three as "possible but less certain" areas. Due to limitations in space only a small part of the full analysis behind this selection is presented here. Three different strategies were chosen when analysing the resistivity data (Table 3). One example is given from each of the three approaches.

The section in Fig. 9a is based on data measured with the reservoir empty at time-step 2 and that in Fig. 9b with the reservoir water at the maximum level at time-step 5a. Figure 10a, b show the results at the same stages using joint inversion from a mixed array of gradient and dipole–dipole data. The joint inversion showed larger residuals, probably due to the transient conditions due to rapid changes of water level as the measurements spanned only a few hours. Wenner data were not available for all conditions while the software available could not handle the pole–dipole data. Due to the limited sensitivity towards the

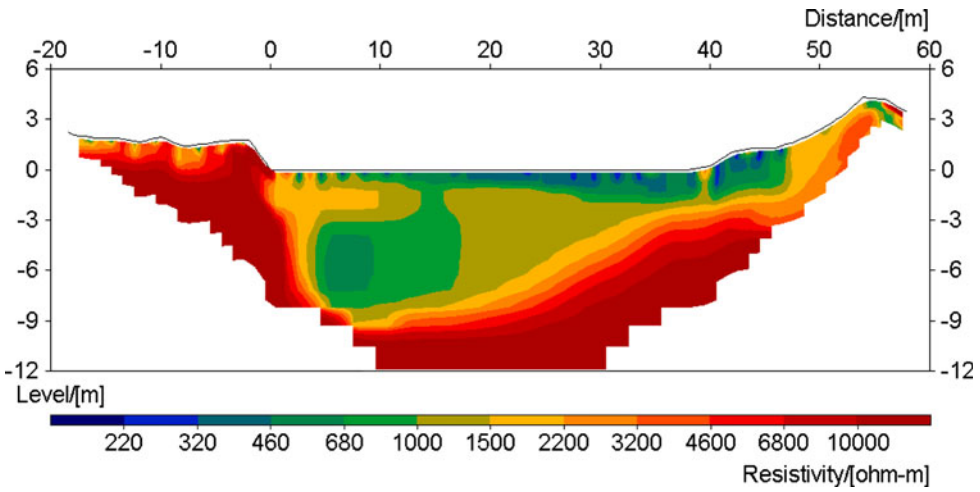

Fig. 8 Inverted resistivity sections based on combined gradient array and Wenner array data from extended line measured with empty reservoir

Table 2 Summary of the results from the resistivity and IP measurements as reported before the locations of the defects were known

Dam section (m)	Observed	Resistivity evaluation method	Level (m)	Comment
7 (5–8)	Several levels	Resistivity at each time alone and difference between levels	367–368	Higher resistivity Faster/larger decrease in res. Decrease in IP
22 (20–24)	All levels and filling #4	Resistivity at each time alone and difference between levels	368–369	Higher resistivity Faster/larger decrease in res. Decrease in IP
27 (25–29)	Filling #2 and filling #3	Difference between levels and between time steps	365–367	Faster/larger decrease in res. Decrease in IP
Possible, but less certain result.				
16 (15–17)	After fill-up and drainage	Difference between time-steps	369	Faster/larger decrease in res. Decrease in IP
27 (26–28)	Several levels	Resistivity at each time alone	369	Higher resistivity
36 (35–37)	After fill-up and drainage	Difference between time-steps	367–368	Decrease in IP

Three defects were detected and three "possible but less certain" defects. The results of the IP measurements undertaken are not commented on in the present study

Table 3 Three different strategies used when analysing the resistivity data

1. *Straightforward analysis*.

Each data set were analysed separately for anomalous zones in the inverted sections. An interesting way to analyse data where low horizontal variations are expected is to subtract the average resistivity of each depth level from the inverted model section. However the results/experience indicated it would be very difficult to detect the designed defects using only this method

2. *Relative difference versus water level*.

The data sets recorded at the different reservoir levels were analyzed via time-lapse inversion, where the data set as recorded before the commencement of the first attempt to fill the reservoir (timestep 1) was used as the reference data set. The results are presented as the relative difference between the models

3. *Relative difference versus time*.

A number of measurements were made at the same water filling level but at different times. This included measurement before filling the reservoir and after draining it, which can be expected to show changes in resistivity as a result of (for example) change in water saturation and temperature in the core. These data sets were also analyzed via time-lapse inversion; the results are presented as relative difference

ends of the electrode layout, the depth section is automatically trimmed off at depth on each side. Here, the inclusion of dipole–dipole data is an advantage as depth penetration is greater and the measurements give more information at the ends of the model.

The resistivity in the dam itself has an apparent layered structure: low, intermediate/high, intermediate/low (from bottom to top). The low resistivity in the bottom layer is probably showing the combined effect of the clay layer used to seal the bottom, plus the water saturated core, filter and rock fill at the lower levels. The method's resolution does not make it possible to discriminate between these parts with the electrodes placed along the top of the core alone. At section 5–7 m (Figs. 9, 10), a high resistive anomaly is visible at 2–3 m depth, which may be associated with the expected leakage zone. Furthermore, around section 22 m a high resistivity anomaly is located at a shallow depth (Figs. 9a, 10a). All anomalies, whether low or high resistivity, indicate inconsistent material properties and may therefore be associated with leakage zones.

Figure 11 shows the changes in resistivity obtained from the gradient array. It would be anticipated that a leakage zone which responds more quickly to a higher reservoir level would be indicated as a zone with large differences in the resistivity measurements. The section in Fig. 11a shows the change resulting from the drop in water level at the start of the experiment at time-step 1 to the completely empty reservoir at time-step 2 (the first attempt to fill it that failed). Little change is shown, although there is a slight drop in resistivity in the upper 3 m, which may be caused by increased moisture content resulting from the attempt to fill the reservoir. Two zones centred around 7–8 and 29–30 m at the mid-lower parts of the section indicate a slightly larger drop in resistivity which may be indicative of anomalous material properties and possible leakage that would give a faster response with higher moisture content and increased temperature. The increase in resistivity at the deeper levels may be a result of the drop in reservoir water level.

When the reservoir water level rises to +2 m (time-step 3), most of the dam section below 2 m below the crest exhibits a drop in resistivity of 10–20% (Fig. 11b), except in two zone (section 27 and 7–8 m) where the drop is over 40%, which may indicate potential leakage zones. Two

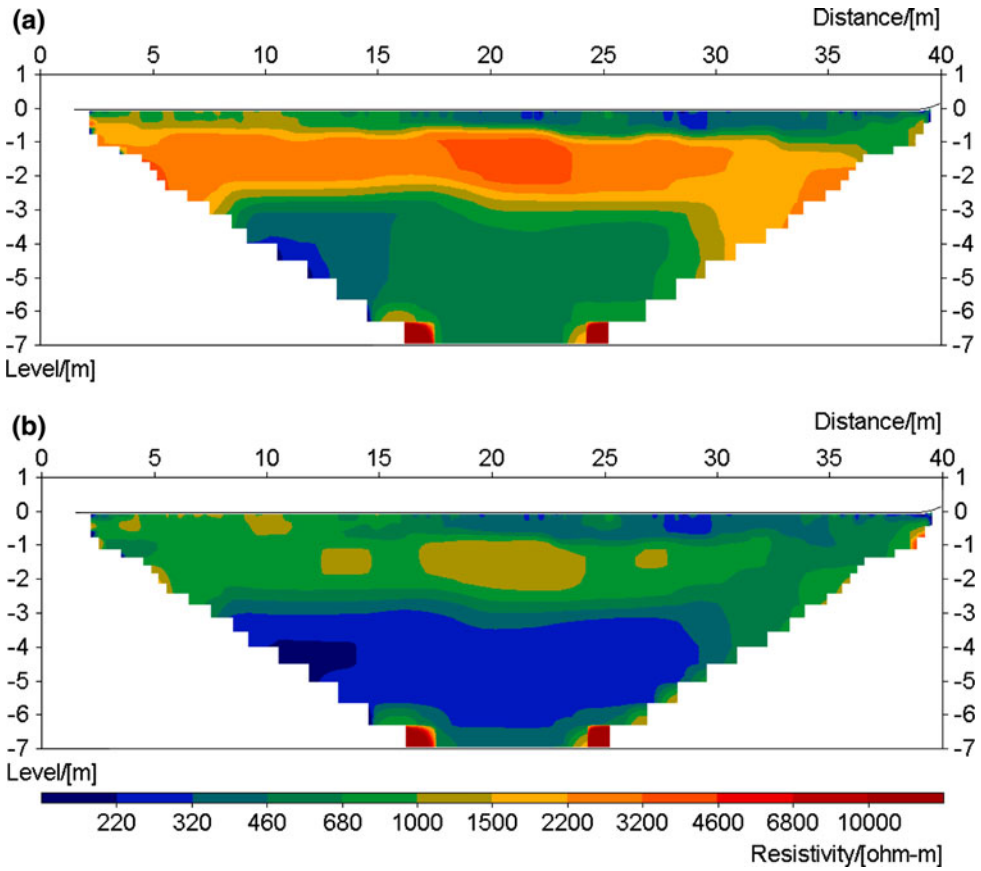

Fig. 9 Inverted resistivity sections. **a** Gradient array at empty reservoir at time-step 2 (mean residual 1.8%). **b** Gradient array at high reservoir level at time-step 5a (mean residual 2.2%)

zones at 1–2 m depth centred around sections 22 and 27 m, corresponding to previously identified high resistivity zones (Fig. 9), showed an unexpected increase in resistivity. At time-step 4, with water at +3.5 m, there was a 40–50% decrease in resistivity compared with the start conditions, for depths below 2 m below dam crest (Fig. 11c) while section 8 m and section 27 m showed a larger decrease (>60%). At time-step 5a, the final rise in water level, there was a drop in resistivity of more than 60% in most sections below 0.5 m depth (Fig. 11d), except section 10–15 m where the drop was between 40 and 50%. At the centre of the dam (section 20 m) however, there was hardly any increase at the bottom of the section, a tendency that could also be observed in the previous two time steps.

A number of measurements were made at the same water filling level but at different times. The result for the difference between time-step 7 and time-step 1 at empty reservoir is shown in Fig. 12a. A decrease in resistivity of around 40–60% in the shallow part (0.5–3 m depth) is clear. This change is quite consistent, except around sections 7 and 16 m where the change is >60%. The overall change is interpreted as caused by increased moisture content following wetting of the embankment dam when the water level increased while the zones with a larger change may indicate anomalous material properties. Below 2.5–3 m depth the resistivity increased, indicating that the moisture content was already high in that area (as discussed above for Fig. 11a), except above c. section 24 m where there is a decrease in resistivity. A similar pattern is seen in the two data sets recorded at reservoir level 1.6 m below dam crest, time-step 6 and time-step 4 (Fig. 12b). One major difference, however, is that the resistivity has increased throughout the lower part of the inverted section. The overall pattern is quite similar for the difference between the recording made immediately after raising the reservoir to its maximum level (time-step 5a) and the measurement made a few hours later (time-step 5b), i.e. a decrease in resistivity in the very top and an increase below (Fig. 12c). The decrease in the top is interpreted as an increase in water saturation in the core during the period following the fill-up.

Discussion

Lessons from the pre-study

The pre-study investigated the degree to which the depth, geometry and resistivity contrast associated with a defect influenced the size of the geophysical anomaly. The

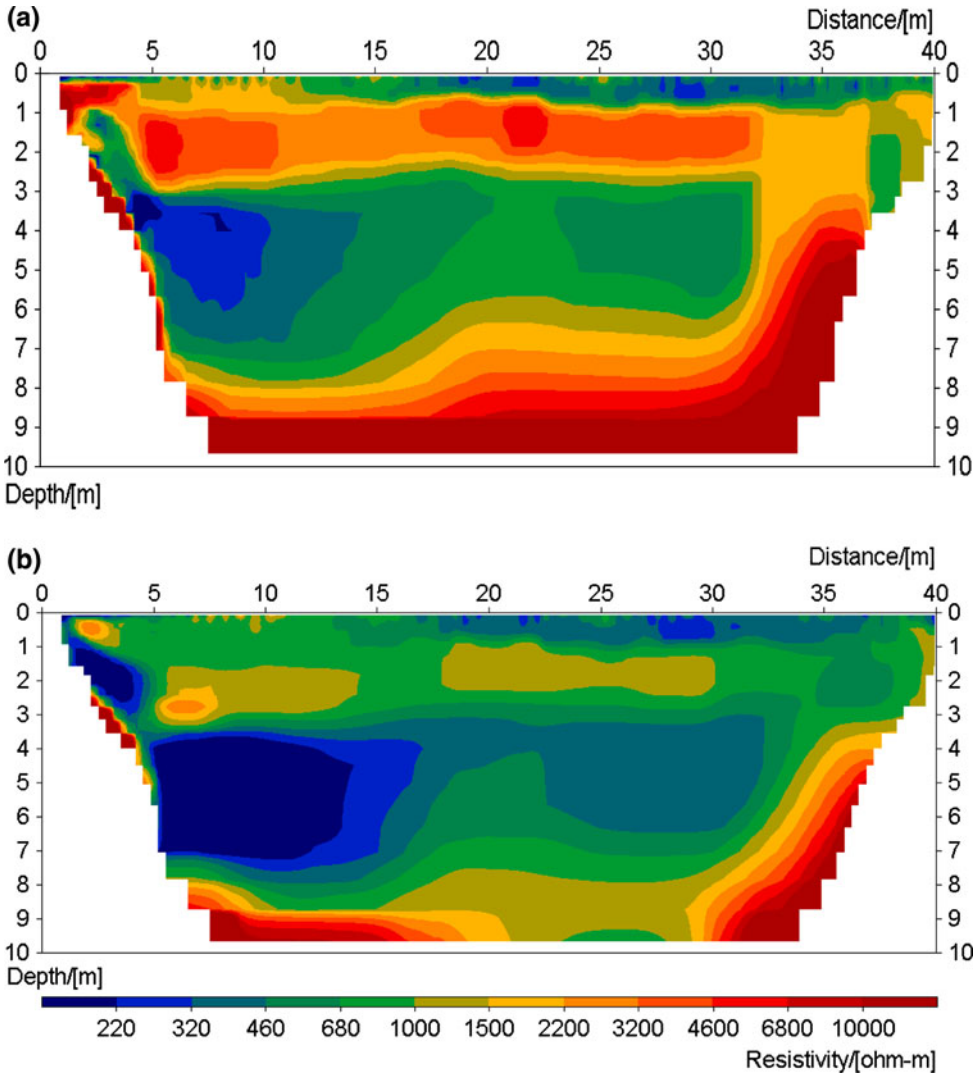

Fig. 10 Inverted resistivity sections. **a** Mixed array at empty reservoir at time-step 2 (mean residual 7.8%). **b** Mixed array at high reservoir level at time-step 5a (mean residual 13.0%)

resistivity contrast was kept unchanged. However, few data were available on the resistivity of soil materials used for the dam construction. Unfortunately, in this pre-study it was not possible to undertake a thorough laboratory analysis of soil samples or in situ measurements at representative sites.

As expected, the size of the defect, but not the shape, had a strong influence on the size of the anomaly. The medium size defect (0.25 m^2) was the smallest which was detected. Closer electrode spacings might improve the resolution of smaller defects. The depth to the defect is important; relatively shallow defects are both more difficult to detect and tend to be smeared out.

The modelling only took into account changes in material properties; temperature-induced variations in resistivity or other transient factors were not considered, although it is known that the resistivity of the soil material decreases significantly with increasing temperature as the mobility of the ions increases (e.g. Ward 1990). In addition, as the changes caused by the anomalous zones are quite small, it is difficult to detect zones of leakage with measurements carried out at a single point in time. On the other hand, a temperature variation will add temporal variation to the resistivities, which is not restricted to the defect area itself but will also affect a volume around the anomalous zone. This significantly increases the possibility of detecting zones of anomalous leakage (Johansson and Dahlin 1996) and is being further investigated.

Field deviations from the pre-study conditions

As noted above, the pre-study concluded that medium sized defects (0.25 m^2) could only be detected above 1 m depth while large defects (1.0 m^2) could be detected at depths of up to 5 m. The constructed defects were designed with a cross-sectional area of 0.16 m^2, i.e. smaller than the medium size used in the pre-study. One defect was located at 3 m depth and two defects on 5 m depth. As a

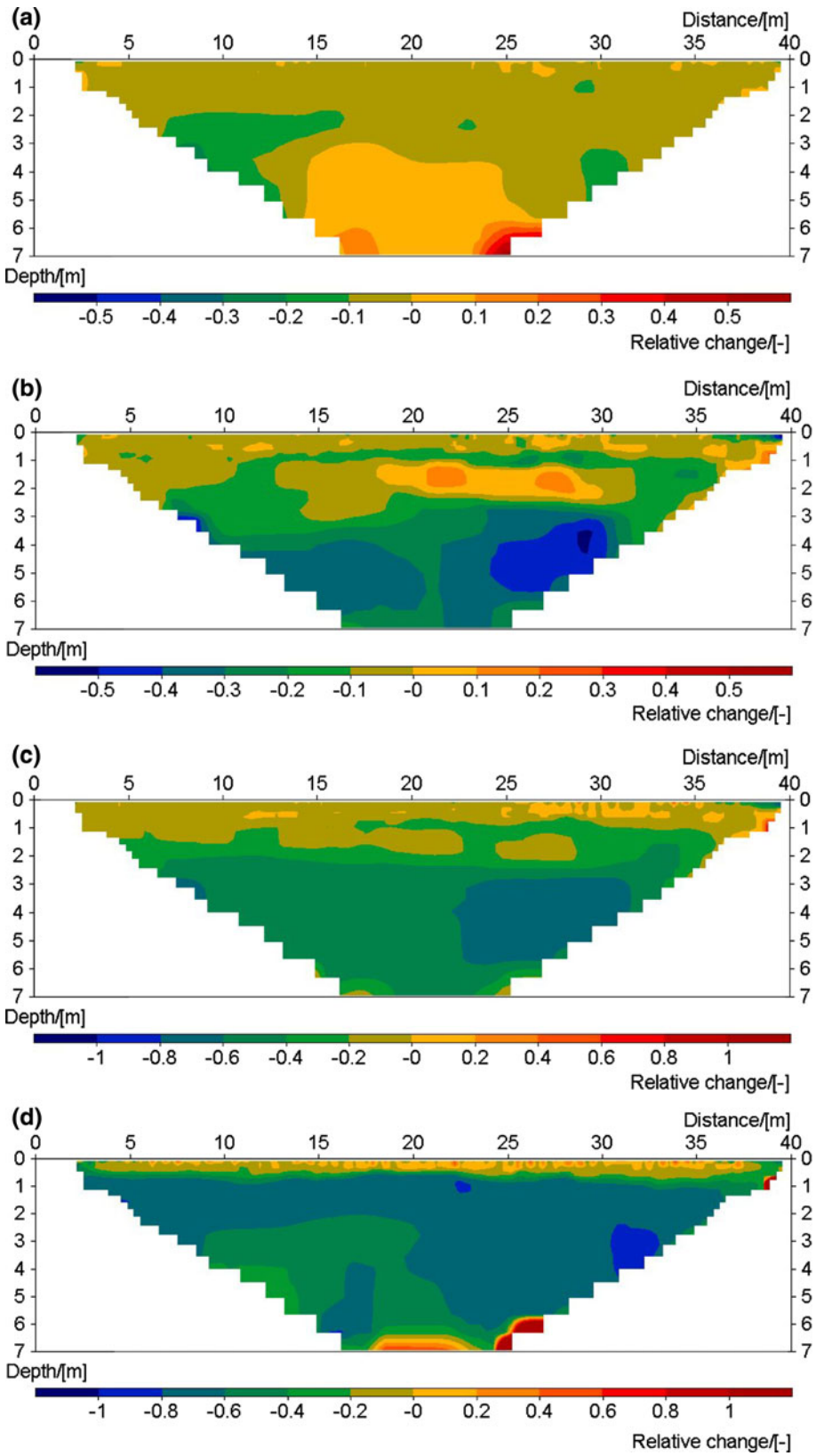

Fig. 11 Difference in inverted resistivity sections based on gradient array: **a** between time-step 2 and time-step 1, **b** between time-step 3 and time-step 1, **c** between time-step 4 and time-step 1, **d** between time-step 5a and time-step 1. Note difference in scale between the sections

consequence, none of the defects were detectable from the pre-study. The group responsible for the construction of the defects considered that larger defects would result in too obvious leakages for the materials used to construct the defects. Moreover, the pre-study only evaluated single measurements, whereas the real situation included the

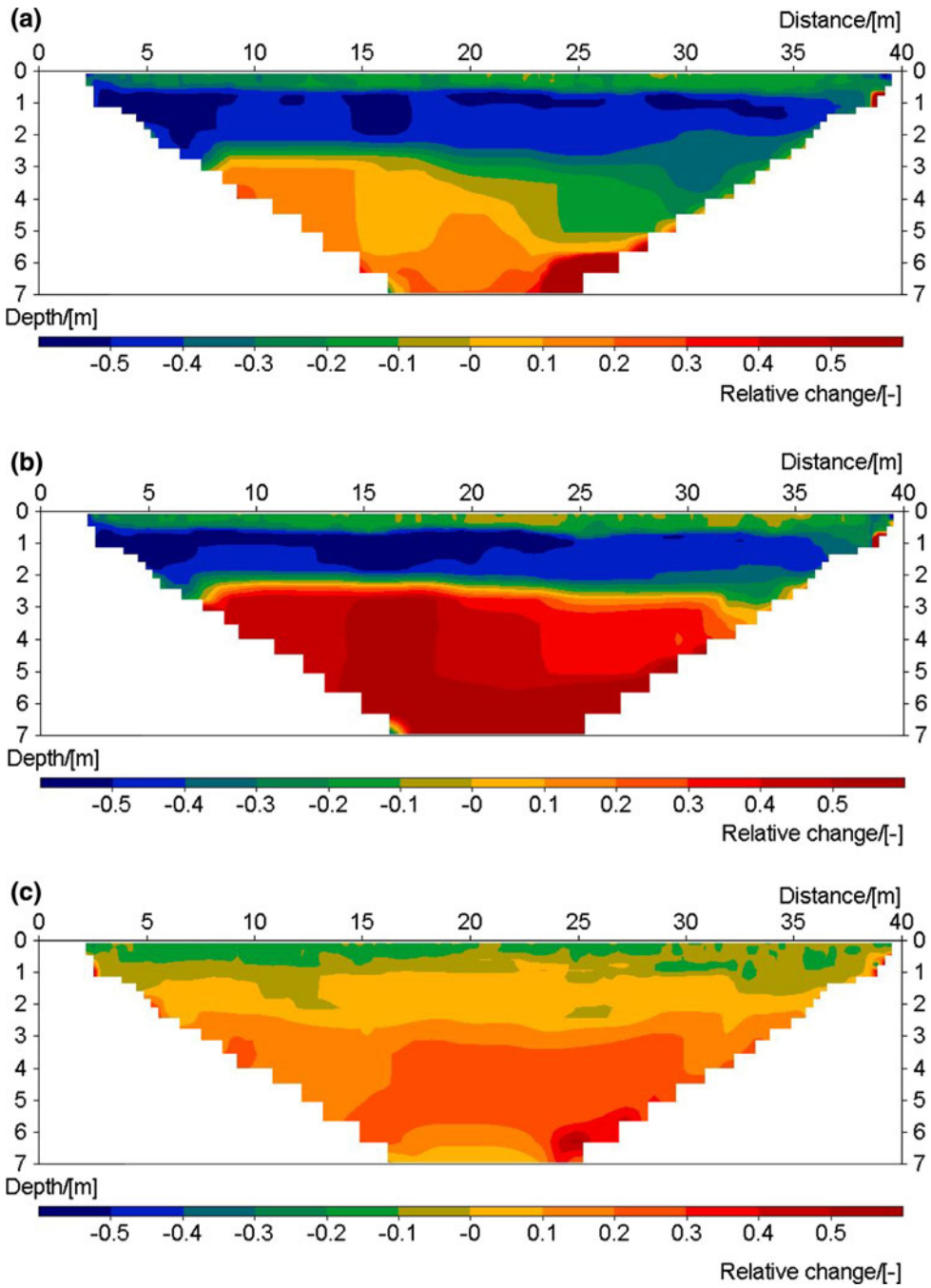

Fig. 12 Difference in inverted resistivity sections based on gradient array data: **a** at empty reservoir between time-step 7 and time-step 2, **b** between time-step 6 and time-step 4, **c** at high reservoir level between time-step 5b and time-step 5a

possibility of repeating the measurements with varying reservoir levels, thereby improving the monitoring conditions.

In the constructed dam there were a number of factors which differed from the pre-study conditions. The most important was the possibility of repeating the measurements over a 1-week period allowing variations over time and with different reservoir levels to be monitored such that anomalies in both space and time could be searched for. Furthermore, the possibility of filling up the reservoir and emptying it while conducting measurements provided an unusual and valuable opportunity rarely available in real dam investigation situations, where only a limited drop in reservoir level is realistic and over a longer time period.

Another important factor was the excellent electrode contact, which in combination with the short electrode separations (0.67 m compared with 1 m) resulted in very good quality data.

On the other hand, some conditions were less favourable in the constructed dam, e.g.

(a) The resistivity of the reservoir water was lower than assumed in the pre-study which reduced the contrast between the water saturated defect zones and the surrounding core material.
(b) The resistivity of the unwashed downstream support fill appeared to be lower than expected in the pre-study, making the desired channelling effect of the current into the dam core less influential.
(c) The clay used for sealing the rock foundation was not anticipated in the pre-study. The clay would be expected to have a very low resistivity, thereby constituting a very conductive layer at the bottom of the dam. The increased contrast in resistivity compared with the rock decreases the resolution achievable by the method in this zone.
(d) Quite large metal objects were found in the dam fill and the core, some visible from the surface. In view of the relatively small anomalies expected from the defects, any metal objects would have a very serious effect.

It is also likely that the transient processes in the materials indicated in the field and in preliminary laboratory tests (Johansson et al. 2005b) will have affected the results. This was not foreseen in the pre-study as the possibility of repeating measurements was not really considered at that time. However, as the construction of the core from compacted glacial till was finished only a few days before measurements commenced, it is likely that conditions for temperature and ion content were changing significantly during the measurement period. One possible explanation for the observed increase in resistivity from one time step to another could be that excess ions were present in the core material; the resistivity would increase when the original pore water has been washed out by the reservoir water with a lower ion content.

Another mechanism which could contribute to the increase in resistivity is washout of fines in the upstream support fill. It was observed during the filling of the reservoir that fine material migrated out into the reservoir water. Other time-dependent changes in the electro-chemical system, possibly affected by change in pore water pressure, could also have had an effect. However, any such effects would occur for only a short period after the construction of a dam and would not be an issue for existing dams.

It should be pointed out that for the gradient array sections presented here, it took about 45 min to record one section and that the resistivity measurements were not initiated immediately after filling up to a new level as SP monitoring was in progress at that time. As a consequence, fast changes could not be recorded, hence it is likely that the differences recorded were unrealistically low. Measuring would have been significantly faster if only resistivity and no IP effects were measured. It is also reasonable to expect that a gradual increase in resistivity would have been detected if monitoring had continued with a full reservoir for a day or more. The fast change in resistivity that is recorded (e.g. the two data sets within a few hours at maximum reservoir level) complicates the evaluation of data combined from different electrode arrays—it took several hours to measure a full combined data set comprising the gradient, dipole–dipole and pole–dipole arrays. For this reason the evaluation of all data sets together through joint inversion has deliberately been avoided. These types of effects are specific to this experiment and would normally not be of concern in monitoring embankment dams.

Comparison of resistivity results and actual defect locations

After analysing the results, three areas were suggested as defect areas and another three as "possible but less certain" defect areas (Table 2). These areas are shown in Figs. 13 and 14, together with the actual locations of the defect in the dam section. No attempt was made to correct for the expected depth distortions associated with 3D-effects, hence it would be expected that the suggested defect areas would be higher than the real defects.

The best agreement is found for Defect B using a monitoring approach. Another predicted defect area is close to Defect A. The depth is similar, but the horizontal location is about one metre away. The horizontal location is normally easier to determine, but the very small resistivity anomalies in this case may have influenced the interpretation. Defect C was not detected by the measurements. It is also probable that the leakage around the pipes, which was observed in the field, was detected, even though the depth was not correct. This anomaly was observed in

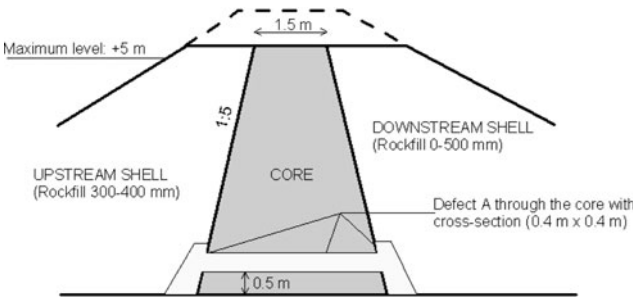

Fig. 13 As-built cross section with depth location and size of the pre-designed built-in defect A (0.4 m × 0.4 m); the defect material consists of sandy gravel. Defect B (1.1 m × 0.15 m) is located on the same level, and defect C (0.4 m × 0.4 m) is located 2 m higher. See also Fig. 14 for defect locations

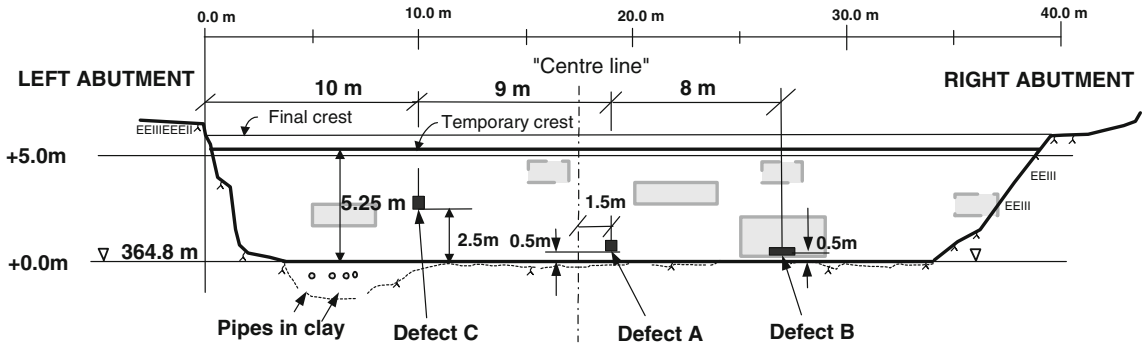

Fig. 14 Result from the resistivity investigations compared with the real location of the defects. Interpreted defect areas from the resistivity investigations are marked with *lines*. Areas classified as "possible but less certain" are marked with *dashed lines*

the outer part of the resistivity image where the result is less certain due to the lower sensitivity of the measurement layouts.

The "possible, but less certain" areas do not match with any of the defects, and may be explained by small variations in the soil properties, or by any of the disturbing factors mentioned above, e.g. transient conditions, metal objects or the placement of clay.

Conclusions

All the defects built into the test dam were small, none being detectable according to the predictions from the pre-study resistivity modelling. However, the pre-study assumed an investigation approach with only standard analysis of single-time measurements. Due to the possibility of comparing measurements at different times and with different water levels in the reservoir, a short-term monitoring approach could be adopted that increased the detection level.

Three defects were constructed carefully, but an additional fourth undesired leakage area occurred around the drainage pipes (Fig. 14), with a similar leakage flow to the three planned defects. The location of the original defects was documented by a design group and not known to the monitoring group during measurement, evaluation and interpretation of the field data.

Of the original three defects, one was identified, one was suggested close to the actual location and one was not detected. This is better than expected from the results of the pre-study. For Defect A, all methods used in the test (temperature, resistivity, SP) indicated a defect area about 2 m to the right of the actual defect. Due to the heterogeneity of the material in the lower part of the downstream fill, a deviation from the basic water flow direction (upstream – downstream) cannot be excluded. Defect B was found by the monitoring approach, despite its depth. Defect C was not detected. However, the additional fourth leakage area around the drainage pipes was detected by resistivity measurements based on both the investigation and the monitoring approach.

The study indicates that resistivity measurements may be a useful method in investigating leakages, but results from single or short time investigations are difficult to evaluate and less accurate than those obtained during long-term monitoring.

Acknowledgments We would like to thank Dr. Johan Friborg for extensive assistance carrying out the field survey, and Dr. Bing Zhou for letting us use his forward resistivity modeling software. We also appreciate the financial support from BC Hydro in Canada, Elforsk AB in Sweden and EBL represented by Statkraft Grøner in Norway who jointly conducted a research project in order to test the performance of geophysical methods at the unique test site at Røssvatn in Norway.

References

Archie GE (1942) Electrical-resistivity log as an aid in determining some reservoir characteristics. Trans AIME 146:54–62

Armbruster H, Brauns J, Mazur W, Merkler GP (1989) Effect of leaks in dams and trials to detect leakages by geophysical means. In: Merkler GP et al (eds) Lecture notes in earth sciences, detection of subsurface flow phenomena, vol 27. Springer, Berlin, pp 3–18

Bergström J (1998) Geophysical methods for investigating and monitoring the integrity of sealing layers on mining waste deposits, Licentiate Thesis, Luleå University of Technology, Luleå, Sweden, ISSN: 1402-1757 ISRN: LTU-LIC–98/24–SE, 77p

Buselli G, Lu K (2001) Groundwater contamination monitoring with multichannel electrical and electromagnetic methods. J Appl Geophys 48:11–23

Butler DK, Llopis JL (1990) Assessment of anomalous seepage conditions. In: Ward S (ed) Investigations in geophysics no. 5: Geotechnical and Environmental Geophysics, vol II. Society of Exploration Geophysicists, Tulsa, pp 153–73

Corwin RW, Butler DK (1989) Geotechnical applications of the self-potential method, report 3, development of self-potential intepretation techniques for seepage detection: Technical report REMR-GT-6, US Army Corps of Engineers, Washington, DC

Dahlin T, Zhou B (2006) Gradient array measurements for multi-channel 2D resistivity imaging. Near Surf Geophys 4:113–123

Dornstädter J (1997) Detection of internal erosion in embankment dams. In: Proceedings of international commission on Large Dams (ICOLD) 19th Congress, Q.73, R.7, Florence

Fell R, Wan CF, Cyganiewicz J, Foster M (2003) Time for development of internal erosion and piping in embankment dams. J Geotech Geoenviron Eng, ASCE 127(4):307–314

Foster M, Fell R, Spannagle M (2000a) The statistics of embankment dam failures and accidents. Can Geotech J 37:1000–1024

Foster M, Fell R, Spannagle M (2000b) A method for assessing the relative likelihood of failure of embankment dams by piping. Can Geotech J 37:1025–1061

Høeg K, Løvoll A, Vaskinn KA (2004) Stability and breaching of embankment dams; field tests on 6 m high dams. Int J Hydropower Dams 11(1):88–92

ICOLD (1995) Dam failures statistical analysis. International Commission on Large Dams (ICOLD), Bulletin 99

ICOLD (1998) World register of dams. International Commission on Large Dams (ICOLD), Paris

Johansson S (1991) Localization and quantification of water leakage in ageing embankment dams by regular temperature measurements. In: Proceedings of international commission on large dams (ICOLD), 17th Congress, Q.65, R.54, Vienna

Johansson S (1997) Seepage monitoring in embankment dams. Doctoral Thesis, TRITA-AMI PHD 1014, ISBN 91-7170-792-1, Royal Institute of Technology, Stockholm

Johansson S, Dahlin T (1996) Seepage monitoring in an earth embankment dam by repeated resistivity measurements. Euro J Environ Eng Geophys 1:229–247

Johansson S, Friborg J, Dahlin T, Sjödahl P (2005a) Long term resistivity and self potential monitoring of embankment dams—experiences from Hällby and Sädva dams, Sweden, Report 05:15. http://www.elforsk.se

Johansson S, Nilsson Å, Garner S, Dahlin T, Friborg J, Sjödahl P (2005b) Internal erosion detection at the Rösvatn test site—experiences from blind test using resistivity, self potential, temperature and visual inspection, Elforsk, Report 05:42. http://www.elforsk.se

Kappelmeyer O (1957) The use of near surface temperature measurements for discovering anomalies due to causes at depths. Geophys Prospect 3:239–258

Loke MH (2001) Constrained time-lapse resistivity imaging inversion. In: Proceedings of SAGEEP 2001. Symposium on the Application of Geophysics to Engineering and Environmental Problems, Denver, Colorado

Loke MH (2002) Rapid 2-D resistivity & IP inversion using the least-squares method. Manual for Res2dinv. http://www.geoelectrical.com, 48p

Loke MH, Acworth I, Dahlin T (2003) A comparison of smooth and blocky inversion methods in 2-D electrical imaging surveys. Explor Geophys 34(3):182–187

Merkler GP, Blinde A, Armbruster H, Döscher HD (1985) Field investigations for the assessment of permeability and identification of leakage in dams and dam foundations. In: Proceedings of international commission on large dams (ICOLD), 15th Congress, Q.58, R.7, Lausanne

Ogilvy AA, Ayed MA, Bogoslovsky VA (1969) Geophysical studies of water leakage from reservoirs. Geophys Prospect 17:36–62

Panthulu TV, Krishnaiah C, Shirke JM (2001) Detection of seepage paths in earth dams using self-potential and electrical resistivity methods. Eng Geol 59:281–295

Schön J (1996) Physical properties of rocks: fundamentals and principles of petrophysics. Handbook of geophysical exploration: vol. 18. Redwood Books, Trowbridge

Schopper JR (1982) Electrical conductivity of rocks containing electrolytes. In: Landolt-Börnstein, Group V, vol 16. Physical Properties of Rocks. Springer, pp 276–291

Sjödahl P, Dahlin T, Johansson S (2005) Using resistivity measurements for dam safety evaluation at Enemossen tailings dam in southern Sweden. Environ Geol 49:267–273

Sjödahl P, Dahlin T, Zhou B (2006) 2.5D Resistivity modeling of embankment dams to assess influence from geometry and material properties. Geophysics 71:107–114

Titov K, Lokhmanov V, Potapov A (2000) Monitoring of water seepage from a reservoir using resistivity and self polarization methods: case history of the Petergoph fountain water supply system. First Break 18:431–435

Triumf C-A, Thunehed H (1996) Two years of self-potential measurements on a large dam in northern Sweden. In: Proceedings of repair and upgrading of dams, KTH, Stockholm, pp 307–315

Van Tuyen D, Canh T, Weller A (2000) Geophysical investigations of river dikes in Vietnam. Eur J Environ Eng Geophys 4:195–206

Ward SH (1990) Resistivity and induced polarization methods, in investigations. In: Ward S (ed) Geophysics no. 5: geotechnical and environmental geophysics, vol I. Society of Exploration Geophysicists, Tulsa, pp 147–189

Wilt MJ, Corwin RF (1988) Numerical modeling of self-potential anomalies due to leaky dams: model and field examples. In: Merkler GP et al (eds) Lecture notes in earth sciences, detection of subsurface flow phenomena, vol 27. Springer, Berlin, pp 73–89

Zhou B, Greenhalgh SA (2001) Finite element three-dimensional direct current resistivity modelling: accuracy and efficiency considerations. Geophys J Int 145:679–688